



X-Ray Constrained Wave Functions: Fundamentals and Effects of the Molecular Orbitals Localization

Alessandro Genoni, Benjamin Meyer

► To cite this version:

Alessandro Genoni, Benjamin Meyer. X-Ray Constrained Wave Functions: Fundamentals and Effects of the Molecular Orbitals Localization. *Advances in Quantum Chemistry*, 2016, 73, pp.333-362. 10.1016/bs.aiq.2015.05.008 . hal-02196473

HAL Id: hal-02196473

<https://hal.univ-lorraine.fr/hal-02196473>

Submitted on 27 May 2020

HAL is a multi-disciplinary open access archive for the deposit and dissemination of scientific research documents, whether they are published or not. The documents may come from teaching and research institutions in France or abroad, or from public or private research centers.

L'archive ouverte pluridisciplinaire **HAL**, est destinée au dépôt et à la diffusion de documents scientifiques de niveau recherche, publiés ou non, émanant des établissements d'enseignement et de recherche français ou étrangers, des laboratoires publics ou privés.

X-Ray Constrained Wave Functions: Fundamentals and Effects of the Molecular Orbitals Localisation

Alessandro Genoni^{*,†,‡} and Benjamin Meyer^{†,‡}

*CNRS, Laboratoire SRSMC, UMR 7565, Vandoeuvre-lès-Nancy, F-54506, France, and
Université de Lorraine, Laboratoire SRSMC, UMR 7565, Vandoeuvre-lès-Nancy, F-54506,
France*

E-mail: Alessandro.Genoni@univ-lorraine.fr

Phone: +33 (0)3 83 68 43 77. Fax: +33 (0)3 83 68 43 71

^{*}To whom correspondence should be addressed

[†]CNRS

[‡]Université de Lorraine

Abstract

The determination of wave functions from experimental data is an appealing objective that has stimulated many researchers over the years. Among the different strategies developed to accomplish this task, the X-ray constrained wave function fitting proposed by Jayatilaka is probably the most promising and it is currently used to determine experimental electron distributions in crystals. To directly introduce an easy chemical interpretability in terms of the traditional Lewis molecular picture without resorting to *a posteriori* techniques, this approach has been recently extended in order to obtain molecular orbitals strictly localised on small molecular fragments (e.g. atoms, bonds or functional groups). In this paper, after reviewing in detail both the historical development of the "experimental" wave function methods and the theoretical foundations of the X-ray constrained wave function techniques, for the first time, we analyse the effect of introducing an *a priori* localisation of molecular orbitals in the framework of Jayatilaka's approach. Our results mainly show that, when large and flexible basis-sets are used in the calculations, the influence of the strong initial assumption represented by the pre-defined localisation is efficiently limited by the information provided by the experimental data.

Keywords: X-ray constrained wave function; Extremely Localised Molecular Orbitals; electron density; localisation; X-ray diffraction.

Introduction

Two great families of quantum mechanical techniques are generally used to compute the physical properties of molecular and crystalline systems: the *ab initio* wave function-based methods and the Density Functional Theory (DFT) strategies. While the former group comprises a series of techniques able to provide wave functions corresponding to increasingly sophisticated and accurate approximations of the Schrödinger equation solutions, the latter relies on the Hohenberg & Kohn theorem¹ according to which the electron density is a crucial physical quantity allowing to determine all the ground state properties of physical systems.

However, although not very well known in the quantum chemistry community, a plausible alternative to the *ab initio* and DFT techniques exists: the approach of the experimentally constrained wave functions or density matrices. These strategies can be considered as semi-empirical methods in which an assumed form for the wave function (or the density matrix) of the systems is fitted to experimental measurements according to some well-defined procedures. There are no limitations in the choice of the experimental data to accomplish this task, even if the X-ray diffraction measurements are the most commonly used both for their generally large abundance and, especially, for their direct connection to the electron density. For this reason these techniques are better known as X-ray constrained wave function strategies.

There are mainly three reasons why this theme has been an active research field for about fifty years. The most important one is the necessity to recap all the experimental observations into an object of unquestionable physical meaning. In this sense, the wave function is the best available theoretical option since in quantum mechanics it is the fundamental entity that intrinsically contains all the information about a physical system. As a consequence, unlike other arbitrary chosen model-objects (e.g., the multipole expansions^{2–4}), an experimentally constrained wave function also enables to compute many properties that are not directly related to the ones used to determine the wave function itself.

Furthermore, it is worth pointing out that extracting an "experimental" wave function

can be extremely useful in all those cases in which it is not possible to perform highly accurate quantum chemistry calculations. In those situations, the available approximate wave functions may provide values of physical properties that deviate from the observed data and, therefore, directly obtaining a wave function from experimental measurements is a powerful technique at our disposal.

Finally, restricting our discussion to the case of constraints consisting in X-ray diffraction data, another crucial reason for determining "experimental" wave functions is represented by the possibility of investigating the Hohenberg & Kohn mapping between electron densities and ground-state wave functions. Of course, solving this mapping problem would be of paramount importance since it would finally allow to perform quantum mechanical calculations exploiting only the simple three-dimensional electron density function.

The first attempt to extract a wave function from experimental measurements dates back to about fifty years ago when Mukherji and Karplus⁵, using experimental values for the dipole moment and the electric field gradient of the hydrofluoric acid, proposed a perturbation approach to constrain a single Slater determinant wave function. Similar techniques have been afterwards exploited to perform calculations on lithium hydride^{6,7}, while Chong and Rasiel tried to extend the constraint procedure through non-perturbative strategies⁸.

Nevertheless, a milestone in this area of interest is represented by the series of pioneering papers published by Clinton and coworkers since 1969^{9–15}. In those studies they have devised original methods to mainly extract idempotent one-particle density matrices from theoretically generated density data. These techniques have been improved over the years, for example extending the original strategy to the case of open-shell single determinant wave functions¹⁶ or introducing a steepest descent algorithm to solve the problem of simultaneously fulfilling the idempotency conditions and the desired agreement with the experimental measurements¹⁷. In this context, Frishberg and Massa¹⁶ have obtained interesting results using high-quality theoretically determined X-ray structure factors to fit the wave functions for simple atomic and molecular systems. Their main conclusion was that the determina-

tion of one-electron properties improved over variational calculations, although that was not observed for the two-electron ones. However, concerning this family of techniques, the most significant result has been obtained by Massa *et al.*¹⁸ that have extracted the idempotent density matrix of beryllium directly exploiting experimental X-ray diffraction data for the first time.

A more recent variant of the Clinton's strategy has been introduced by Howard and coworkers¹⁹ that resorted to a simulated annealing technique to fit single determinant wave functions of much larger systems, such as methylamine and formamide. In this context it is also important to cite the study conducted by Snyder and Stevens²⁰ that obtained the experimental idempotent density matrix for the azide ion in crystalline potassium azide. In particular, they have shown that the electron deformation density maps constructed from the fitted density matrices present some features that can be found in the corresponding theoretical densities, but that are not generally observable in multipole model charge distributions. Finally, in this class of strategies another noteworthy technique is the X-ray Atomic Orbital (XAO) method proposed by Tanaka^{21,22} that mainly aims at modelling the distortion of the heavy-atoms atomic orbitals due to the crystal-field effects.

Nevertheless, an intrinsic and important limitation of all the previous Clinton-like techniques is their only focus on the use of idempotent density matrices (namely, single Slater determinant wave functions). To overcome this serious drawback, Hibbs, Waller and coworkers^{23,24} have recently devised a new interesting method in which the occupation numbers of predetermined (occupied and virtual) Molecular Orbitals are optimised through a fitting to experimental structure factors. The MOON (Molecular Orbitals Occupation Numbers) approach is potentially linear scaling and it is also characterised by an advantageous ease of properties calculation, even if the pre-computation and selection of Molecular Orbitals could be a serious limit for quite large systems.

In more advanced approaches the simple idempotency requirement has been replaced by the N-representability conditions. As well known, these conditions guarantee that the

density operators come from a valid antisymmetric wave function and, for a one-particle density matrix, they simply correspond to the fact that density matrix eigenvalues must lie between zero and one. In this context, among the N-representable strategies a prominent role is occupied by the methods developed by Weyrich and coworkers^{25–27} and by Gillet and collaborators^{28–30}. In fact, these researchers have interestingly demonstrated over the years that the wealth of information about the chemical bonding effects contained in the inelastic Compton scattering data^{31,32} can be efficiently used to reconstruct one-particle density matrices. Finally, it is worth mentioning the studies performed by Cassam-Chenaï^{33,34} that pointed out the importance of using ensemble N-representable density matrices. In particular, he has proposed to express these one-particle density matrices in terms of a small number of pre-computed *ab initio* wave functions and to afterwards determine few coupling coefficients through a fitting to collected experimental data. The strategy has been applied in connection with polarised neutron diffraction data and it allowed to analyse the magnetisation density of the CoCl_4^{2-} ion in the Cs_3CoCl_5 crystal.

Unfortunately, even introducing N-representability conditions may not be enough. In fact, in 1975 Gilbert³⁵ has shown that, in principle, an infinite number of N-representable one-particle density matrices can reproduce a desired electron density distribution. Therefore, fitting to density data alone, as done in all the previously described strategies, is a necessary but not sufficient criterion to guarantee the determination of physically meaningful experimentally constrained wave functions or density matrices. To overcome this drawback, Henderson and Zimmerman³⁶ have suggested that of all the possible single Slater determinants that are compatible with a given electron density, the optimal one is that which minimises the Hartree-Fock energy. This idea led to another modified Clinton's approach that was applied to lithium hydride using theoretical structure factors. An alternative has been afterwards proposed by Levy & Goldstein³⁷ and by Gritsenko & Zhidomirov³⁸, according to whom, when a given wave function is not univocally determined from the data, the single Slater determinant to be chosen is the one that simply minimises the kinetic energy.

Following this philosophy, Parr and coworkers^{39–41} have devised original strategies to extract Kohn-Sham orbitals using electron density data obtained from theoretical wave functions or quantum Monte-Carlo computations. These strategies are also currently used to generate new DFT functionals.

However, supported by the Levy's constrained search formalism⁴², according to which the exact wave function is the one that minimises the total energy while reproducing a given electron distribution, Jayatilaka^{43–50} has quite recently proposed a more practical implementation of the Henderson & Zimmerman's idea. This novel technique, which is known as X-ray constrained wave function fitting, consists in determining the single Slater determinant that minimises the corresponding energy, but that, at the same time, reproduces a set of experimental structure factor amplitudes within a desired accuracy. In other words, using the Lagrange multiplier technique, the strategy variationally minimises a new functional given by the energy associated with the single Slater determinant and an additional term represented by the statistical agreement with the experimental diffraction data. In particular, the Lagrange multiplier is iteratively increased until the desired agreement between experimental and calculated values is reached.

The Jayatilaka approach is probably the most promising strategy among all the experimentally constrained methods developed so far. In fact, other than giving physically meaningful "experimental" electron distributions, the technique has been also successful in the study of chemical and physical properties such as in-crystal molecular dipole moments, in-crystal polarisabilities and refractive indices^{51,52}. Unfortunately, due to the complete delocalisation of the obtained Molecular Orbitals, the simple chemical interpretability of the resulting charge distributions **is not immediate and, for this reason, Jayatilaka and coworkers have already tried to recover it extracting quantities such as the Electron Localisation Functions (ELFs)⁵³, the Electron Localisability Indicators (ELIs)^{54,55} and the Roby indexes⁵⁶ directly from X-ray constrained wave functions.**

In this context, we have recently proposed an alternative technique^{57–59} to directly include

the traditional Lewis picture of molecules in the X-ray constrained wave function fitting, without using *a posteriori* localisation techniques or analyses. In particular, the new method enables to extract from X-ray diffraction data a single Slater determinant constructed with molecular orbitals strictly localised on small molecular fragments (e.g., atoms, bonds or functional groups) and it can be considered as the combination of Jayatilaka's approach with the technique developed by Stoll⁶⁰ for the *a priori* determination of Extremely Localised Molecular Orbitals (ELMOs). Our previous studies have shown that, provided that good-quality crystallographic data are available, the extraction of X-ray constrained ELMOs is straightforward and that the XC-ELMO strategy is a new and potentially useful tool for the reconstruction and analysis of electron densities from experimental diffraction data^{58,59}.

Concerning the Extremely Localised Molecular Orbitals, it is worthwhile to point out that, unlike the traditional *a posteriori* localisation techniques (e.g. Pipek-Mezey⁶¹, Foster-Boys^{62,63} or Edimiston-Ruedenberg^{64,65}) and analyses (e.g., ELF⁶⁶ or ELI⁶⁷), the usual chemical picture of molecules is obtained only introducing a localisation scheme before performing the calculations. If on the one hand this user-defined pre-localisation can be considered as a strong empirical bias that makes the ELMO technique less general than all the *a posteriori* methods, on the other hand the definition of a localisation pattern allows to obtain Molecular Orbitals that are really strictly localised on molecular subunits, which make them easily transferable from a molecule to another one and, consequently, suitable to be collected in proper libraries to instantaneously reconstruct wave functions or electron distributions of large systems. On the contrary, all the traditional localisation procedures provide Molecular Orbitals that keep orthogonalisation tails beyond the main localisation region, which prevents a direct and harmless transferability. In fact, although small, these tails must be deleted before the transfer and this unfortunately corresponds to a non-negligible perturbation that results in a large increase of the energy of the system^{68,69}.

Although, as just mentioned, the introduction of a predefined localisation is a strong empirical constraint in electronic structure calculations, the effects of using Extremely Localised

Molecular Orbitals in the framework of the X-ray constrained wave function fitting has not been studied yet. Nevertheless, shedding light on this aspect is crucial for the recently proposed XC-ELMO technique since it will allow to evaluate if the presence of experimental diffraction data is able to mitigate the bias represented by the user-defined pre-localisation. Therefore, the objective of this work is dual. On the one side, we will present in detail the basic theory and the capabilities of Jayatilaka's approach and of its recent extension into the ELMOs framework in order to further spread these original methods among the quantum chemistry community. On the other side we will study the effects of the *a priori* localisation on the experimentally reconstructed wave functions and electron densities, analysing both the convergence towards the desired statistical agreement with the collected X-ray diffraction data and the main topological properties of the obtained electron distributions.

Theory

In this section the theory of the X-ray constrained wave function strategies will be described in detail. At first, after focusing on the main assumptions of Jayatilaka's approach, we will present the fundamental equations of the original X-ray constrained Hartree-Fock (XC-HF) method. Afterwards, we will briefly introduce the theory of the recently developed X-ray constrained ELMO (XC-ELMO) technique and, finally, we will discuss important details strictly related to the X-ray constrained calculations.

X-Ray Constrained Wave Function Fitting: Basic Assumptions. Assuming to deal with molecular crystals, let us consider a fictitious crystalline system in which: a) each crystal-unit does not interact with the other ones; b) the global electron density is identical to the one of the real interacting system.

The first assumption allows us to write the global wave function of the crystal as:

$$|\Psi_{\text{cryst}}\rangle = \prod_k |\Psi_k\rangle \quad (1)$$

where all the crystal-unit wave functions $|\Psi_k\rangle$ are formally identical and related to each other through the crystal symmetry operations. The choice of the functional form for $|\Psi_k\rangle$ is completely arbitrary and it can be considered as a further assumption of the technique since it will eventually determine the type of X-ray constrained wave function (e.g., Hartree-Fock, ELMO, CI, MCSCF, etc.) that is desired.

Considering all the non-interacting units as symmetry-unique portions of the crystal unit-cell, the unit-cell electron distribution can be simply computed as sum of N_m crystal-unit charge densities $\rho_k(\mathbf{r})$ that are related to the reference electron density $\rho_0(\mathbf{r})$ through the unit-cell symmetry operations $\{\mathbf{R}_k, \mathbf{r}_k\}$:

$$\rho_{cell}(\mathbf{r}) = \sum_{k=1}^{N_m} \rho_k(\mathbf{r}) = \sum_{k=1}^{N_m} \rho_0(\mathbf{R}_k^{-1}(\mathbf{r} - \mathbf{r}_k)) \quad (2)$$

The charge distribution $\rho_0(\mathbf{r})$ is associated with the wave function $|\Psi_0\rangle$ for the reference unit. Following Jayatilaka, this wave function is obtained not only minimising the energy of the reference crystal-unit, but also reproducing a set of experimental structure factor amplitudes. In other words, $|\Psi_0\rangle$ is the wave function that minimises the following functional:

$$\begin{aligned} J[\Psi_0] &= \langle \Psi_0 | \hat{H}_0 | \Psi_0 \rangle + \lambda (\chi^2 - \Delta) \\ &= E_0[\Psi_0] + \lambda (\chi^2[\Psi_0] - \Delta) \end{aligned} \quad (3)$$

with \hat{H}_0 as the Hamiltonian operator for the reference crystal-unit, λ as the Lagrange multiplier associated with the experimental constraint, Δ as the desired agreement between theoretical and experimental values, and χ^2 as the measure of the statistical agreement between the calculated and the observed structure factor amplitudes $|F_{\mathbf{h}}^{calc}|$ and $|F_{\mathbf{h}}^{exp}|$, namely:

$$\chi^2 = \frac{1}{N_r - N_p} \sum_{\mathbf{h}} \frac{(\eta |F_{\mathbf{h}}^{calc}| - |F_{\mathbf{h}}^{exp}|)^2}{\sigma_{\mathbf{h}}^2} \quad (4)$$

where N_r is the number of considered experimental scattering data, N_p is the number of adjustable parameters (namely, only the Lagrange multiplier λ), \mathbf{h} is the tern of Miller indices labelling the reflection, $\sigma_{\mathbf{h}}$ is the error associated with each measure and η is an \mathbf{h} -independent scale-factor that is determined to minimise χ^2 .

It is crucial to point out that it is the presence of the experimental constraint in functional (3) that allows to fulfil the starting assumption that the global electron density of the fictitious non-interacting system is identical to the one of the real interacting crystal. Of course, the accuracy of the assumption is strictly related to the quality and completeness of the experimental X-ray diffraction data used in the calculations.

The X-Ray Constrained Hartree-Fock Method. Since the XC-HF strategy has been recently extended also to the unrestricted case⁴⁹, for the sake of generality, in this section we will derive the X-ray constrained Hartree-Fock equations in their spin-orbital form. To accomplish this task, let us consider an N -electron system and let us assume that the reference wave function $|\Psi_0\rangle$ is a single Slater determinant built up with a set of N spin-orbitals:

$$|\Psi_0\rangle = \frac{1}{\sqrt{N!}} \hat{A} [\phi_1^0 \phi_2^0 \phi_3^0 \dots \phi_N^0] \quad (5)$$

The XC-HF equations can be simply derived through the minimisation of the functional (3) with respect to the spin-orbitals, subject to the constraint of the spin-orbitals orthonormality. Therefore, omitting any subscripts and superscripts corresponding to the reference crystal-unit, the new functional to be minimised becomes

$$L[\boldsymbol{\phi}] = E[\boldsymbol{\phi}] + \lambda(\chi^2[\boldsymbol{\phi}] - \Delta) - \sum_{i,k=1}^N \epsilon_{ki} (\langle \phi_i | \phi_k \rangle - \delta_{ik}) \quad (6)$$

where $\{\epsilon_{ki}\}$ constitutes a set of Lagrange multipliers and where the symbol $\boldsymbol{\phi}$ stresses the functional dependence on the spin-orbitals.

Now, assuming to work with real spin-orbitals and considering the arbitrary variation of

$L[\phi]$ with respect to the occupied spin-orbital $|\phi_j\rangle$, we obtain

$$\delta_{(\phi_j)} L = \delta_{(\phi_j)} E + \lambda \delta_{(\phi_j)} \chi^2 - 2 \sum_{k=1}^N \epsilon_{kj} \langle \delta\phi_j | \phi_k \rangle \quad (7)$$

where, as well known, $\delta_{(\phi_j)} E$ is

$$\delta_{(\phi_j)} E = 2 \langle \delta\phi_j | \hat{F} | \phi_j \rangle \quad (8)$$

with \hat{F} as the usual Fock operator for the spin-orbital case, while, exploiting the relation $|F_{\mathbf{h}}^{calc}| = [F_{\mathbf{h}}^{calc} (F_{\mathbf{h}}^{calc})^*]^{\frac{1}{2}}$, $\delta_{(\phi_j)} \chi^2$ is

$$\delta_{(\phi_j)} \chi^2 = \frac{\eta}{N_r - N_p} \sum_{\mathbf{h}} \frac{\eta |F_{\mathbf{h}}^{calc}| - |F_{\mathbf{h}}^{exp}|}{\sigma_{\mathbf{h}}^2 |F_{\mathbf{h}}^{calc}|} \left\{ (F_{\mathbf{h}}^{calc})^* \delta_{(\phi_j)} F_{\mathbf{h}}^{calc} + F_{\mathbf{h}}^{calc} \delta_{(\phi_j)} (F_{\mathbf{h}}^{calc})^* \right\} \quad (9)$$

Since the structure factors are Fourier transforms of the unit-cell electron density and given that the structure factor operator is defined as

$$\hat{I}_{\mathbf{h}} = \sum_{k=1}^{N_m} e^{i2\pi(\mathbf{R}_k \mathbf{r} + \mathbf{r}_k) \cdot (\mathbf{B}\mathbf{h})} = \hat{I}_{\mathbf{h},R} + i \hat{I}_{\mathbf{h},C} \quad (10)$$

where \mathbf{B} is the reciprocal lattice matrix and both $\hat{I}_{\mathbf{h},R}$ and $\hat{I}_{\mathbf{h},C}$ (real and imaginary part of $\hat{I}_{\mathbf{h}}$, respectively) are hermitian, we get

$$F_{\mathbf{h}}^{calc} = \sum_{i=1}^N \langle \phi_i | \hat{I}_{\mathbf{h}} | \phi_i \rangle \quad (11)$$

and

$$(F_{\mathbf{h}}^{calc})^* = \sum_{i=1}^N \langle \phi_i | \hat{I}_{\mathbf{h}}^\dagger | \phi_i \rangle \quad (12)$$

Furthermore, bearing in mind that we are working with real spin-orbitals, from equations

(11) and (12), it is easy to obtain

$$\delta_{(\phi_j)} F_{\mathbf{h}}^{calc} = 2 \langle \delta\phi_j \mid \hat{I}_{\mathbf{h}} \mid \phi_j \rangle \quad (13)$$

and

$$\delta_{(\phi_j)} (F_{\mathbf{h}}^{calc})^* = (\delta_{(\phi_j)} F_{\mathbf{h}}^{calc})^* \quad (14)$$

Using equation (14) in (9), $\delta_{(\phi_j)} \chi^2$ becomes

$$\delta_{(\phi_j)} \chi^2 = \frac{2\eta}{N_r - N_p} \sum_{\mathbf{h}} \frac{\eta |F_{\mathbf{h}}^{calc}| - |F_{\mathbf{h}}^{exp}|}{\sigma_{\mathbf{h}}^2 |F_{\mathbf{h}}^{calc}|} \operatorname{Re} \left\{ (F_{\mathbf{h}}^{calc})^* \delta_{(\phi_j)} F_{\mathbf{h}}^{calc} \right\} \quad (15)$$

and, exploiting the definition (10), relation (13) can be written as

$$\delta_{(\phi_j)} F_{\mathbf{h}}^{calc} = 2 \left[\langle \delta\phi_j \mid \hat{I}_{\mathbf{h},R} \mid \phi_j \rangle + i \langle \delta\phi_j \mid \hat{I}_{\mathbf{h},C} \mid \phi_j \rangle \right] \quad (16)$$

Now, substituting equation (16) into (15), we have

$$\delta_{(\phi_j)} \chi^2 = 2 \left\{ \sum_{\mathbf{h}} K_{\mathbf{h}} \operatorname{Re} \left\{ F_{\mathbf{h}}^{calc} \right\} \langle \delta\phi_j \mid \hat{I}_{\mathbf{h},R} \mid \phi_j \rangle + \sum_{\mathbf{h}} K_{\mathbf{h}} \operatorname{Im} \left\{ F_{\mathbf{h}}^{calc} \right\} \langle \delta\phi_j \mid \hat{I}_{\mathbf{h},C} \mid \phi_j \rangle \right\} \quad (17)$$

with

$$K_{\mathbf{h}} = \frac{2\eta}{N_r - N_p} \frac{\eta |F_{\mathbf{h}}^{calc}| - |F_{\mathbf{h}}^{exp}|}{\sigma_{\mathbf{h}}^2 |F_{\mathbf{h}}^{calc}|} \quad (18)$$

and the arbitrary variation of the functional L given by equation (7) becomes

$$\begin{aligned} \delta_{(\phi_j)} L = & 2 \left\{ \langle \delta\phi_j | \hat{F} | \phi_j \rangle + \right. \\ & + \lambda \sum_{\mathbf{h}} K_{\mathbf{h}} \operatorname{Re} \left\{ F_{\mathbf{h}}^{calc} \right\} \langle \delta\phi_j | \hat{I}_{\mathbf{h},R} | \phi_j \rangle + \\ & + \lambda \sum_{\mathbf{h}} K_{\mathbf{h}} \operatorname{Im} \left\{ F_{\mathbf{h}}^{calc} \right\} \langle \delta\phi_j | \hat{I}_{\mathbf{h},C} | \phi_j \rangle + \\ & \left. - \sum_{k=1}^N \epsilon_{kj} \langle \delta\phi_j | \phi_k \rangle \right\} \end{aligned} \quad (19)$$

Since $\langle \delta\phi_j |$ is arbitrary, the minimum of L , which corresponds to $\delta_{(\phi_j)} L = 0$, is reached when the following relation is fulfilled for each j :

$$\hat{F}^{exp} |\phi_j\rangle = \sum_{k=1}^N \epsilon_{kj} |\phi_k\rangle \quad (20)$$

where the new "experimental" Fock operator, which takes into account the constraint of the experimental structure factor amplitudes, is given by

$$\hat{F}^{exp} = \hat{F} + \lambda \sum_{\mathbf{h}} K_{\mathbf{h}} \operatorname{Re} \left\{ F_{\mathbf{h}}^{calc} \right\} \hat{I}_{\mathbf{h},R} + \lambda \sum_{\mathbf{h}} K_{\mathbf{h}} \operatorname{Im} \left\{ F_{\mathbf{h}}^{calc} \right\} \hat{I}_{\mathbf{h},C} \quad (21)$$

Finally, performing a unitary transformation of the spin-orbitals among themselves and considering the invariance of \hat{F}^{exp} to that transformation, equations (20) transform into the canonical X-ray constrained Hartree-Fock equations:

$$\hat{F}^{exp} |\phi'_j\rangle = \epsilon'_j |\phi'_j\rangle \quad (22)$$

X-Ray Constrained Extremely Localised Molecular Orbitals. Unlike the XC-HF method, the more recent X-ray constrained ELMO strategy has been developed only in the restricted case. For this reason, from now on, we will assume that each crystal-unit is a

$2N$ -electron closed-shell system described by an ELMO wave function, namely, by a single Slater determinant built up with Extremely Localised Molecular Orbitals.

For the sake of simplicity, let us consider the reference crystal-unit and let us subdivide it into f fragments (e.g., atoms, bonds or functional groups) that may overlap. Due to this partition, each subunit is associated with a local basis-set that is constituted by the only basis functions centred on the atoms belonging to the fragment. Therefore, if $\left\{ |\chi_{i\mu}^0\rangle \right\}_{\mu=1}^{M_i^0}$ is the set of atomic orbitals for the i -th subunit, the α -th ELMO of the fragment can be written like this

$$|\varphi_{i\alpha}^0\rangle = \sum_{\mu=1}^{M_i^0} C_{i\mu,i\alpha}^0 |\chi_{i\mu}^0\rangle \quad (23)$$

and the ELMO wave function of the reference unit as

$$|\Psi_{ELMO}^0\rangle = \frac{1}{\det[\mathbf{S}] \sqrt{(2N)!}} \hat{A} \left[\prod_{i=1}^f \prod_{\alpha=1}^{n_i} \varphi_{i\alpha}^0 \bar{\varphi}_{i\alpha}^0 \right] \quad (24)$$

where \mathbf{S} is the overlap matrix between the occupied ELMOs, \hat{A} is the antisymmetrizer, n_i is the number of occupied ELMOs for the i -th subunit, $\bar{\varphi}_{i\alpha}^0$ is a spin-orbital with spatial part $\varphi_{i\alpha}^0$ and spin part β . The overlap matrix arises from the fact that ELMOs localised on different subunits are generally non-orthogonal due to the partial sharing of basis functions between predefined overlapping fragments.

Now, in order to obtain the equations for the XC-ELMO technique, let us minimise the functional (3) with respect to the occupied ELMOs. In particular, let us consider the variation of J associated with the arbitrary variation of the occupied ELMO $|\varphi_{j\beta}^0\rangle$. Omitting all the subscripts and superscripts corresponding to the reference unit, we obtain

$$\delta_{(\varphi_{j\beta})} J = \delta_{(\varphi_{j\beta})} E + \lambda \delta_{(\varphi_{j\beta})} \chi^2 \quad (25)$$

where, similarly to the XC-HF equations, we get

$$\delta_{(\varphi_{j\beta})}\chi^2 = \frac{\eta}{N_r - N_p} \sum_{\mathbf{h}} \frac{\eta |F_{\mathbf{h}}^{calc}| - |F_{\mathbf{h}}^{exp}|}{\sigma_{\mathbf{h}}^2 |F_{\mathbf{h}}^{calc}|} \left\{ (F_{\mathbf{h}}^{calc})^* \delta_{(\varphi_{j\beta})} F_{\mathbf{h}}^{calc} + F_{\mathbf{h}}^{calc} \delta_{(\varphi_{j\beta})} (F_{\mathbf{h}}^{calc})^* \right\} \quad (26)$$

while, following Stoll⁶⁰, we have

$$\delta_{(\varphi_{j\beta})} E = 4 \langle \delta \varphi_{j\beta} | (1 - \hat{\rho}) \hat{F} | \tilde{\varphi}_{j\beta} \rangle \quad (27)$$

with the dual orbital $|\tilde{\varphi}_{j\beta}\rangle$ defined as

$$|\tilde{\varphi}_{j\beta}\rangle = \sum_{k=1}^f \sum_{\gamma=1}^{n_k} [\mathbf{S}^{-1}]_{k\gamma,j\beta} |\varphi_{k\gamma}\rangle \quad (28)$$

and the global density operator $\hat{\rho}$ as

$$\hat{\rho} = \sum_{j=1}^f \sum_{\beta=1}^{n_j} |\tilde{\varphi}_{j\beta}\rangle \langle \varphi_{j\beta}| = \sum_{j=1}^f \sum_{\beta=1}^{n_j} |\varphi_{j\beta}\rangle \langle \tilde{\varphi}_{j\beta}|, \quad (29)$$

As already shown in our previous studies^{57,58}, through a simple mathematical derivation that exploits the definition (10), we obtain

$$\begin{aligned} \delta_{(\varphi_{j\beta})} J &= 4 \left\{ \langle \delta \varphi_{j\beta} | (1 - \hat{\rho}) \hat{F} | \tilde{\varphi}_{j\beta} \rangle + \right. \\ &\quad + \lambda \sum_{\mathbf{h}} K_{\mathbf{h}} \operatorname{Re} \left\{ F_{\mathbf{h}}^{calc} \right\} \langle \delta \varphi_{j\beta} | (1 - \hat{\rho}) \hat{I}_{\mathbf{h},R} | \tilde{\varphi}_{j\beta} \rangle + \\ &\quad \left. + \lambda \sum_{\mathbf{h}} K_{\mathbf{h}} \operatorname{Im} \left\{ F_{\mathbf{h}}^{calc} \right\} \langle \delta \varphi_{j\beta} | (1 - \hat{\rho}) \hat{I}_{\mathbf{h},C} | \tilde{\varphi}_{j\beta} \rangle \right\} \end{aligned} \quad (30)$$

with $K_{\mathbf{h}}$ given by equation (18). Furthermore, since also in this case $\langle \delta \varphi_{j\beta} |$ is arbitrary, the minimum of the functional (corresponding to $\delta_{(\varphi_{j\beta})} J = 0$) is reached when, for all j and β ,

we have

$$\left\{ \begin{aligned} & (1 - \hat{\rho}) \hat{F} + \lambda \sum_{\mathbf{h}} K_{\mathbf{h}} \operatorname{Re} \left\{ F_{\mathbf{h}}^{calc} \right\} (1 - \hat{\rho}) \hat{I}_{\mathbf{h},R} + \\ & + \lambda \sum_{\mathbf{h}} K_{\mathbf{h}} \operatorname{Im} \left\{ F_{\mathbf{h}}^{calc} \right\} (1 - \hat{\rho}) \hat{I}_{\mathbf{h},C} \end{aligned} \right\} | \tilde{\varphi}_{j\beta} \rangle = 0 \quad (31)$$

Now, considering the definition of fragment density operator

$$\hat{\rho}_j = \sum_{\beta=1}^{n_j} | \tilde{\varphi}_{j\beta} \rangle \langle \varphi_{j\beta} | \quad (32)$$

and proceeding as in our original paper⁵⁷, we add

$$|Q\rangle = \left\{ \hat{\rho}_j^\dagger \hat{F} + \lambda \sum_{\mathbf{h}} K_{\mathbf{h}} \operatorname{Re} \left\{ F_{\mathbf{h}}^{calc} \right\} \hat{\rho}_j^\dagger \hat{I}_{\mathbf{h},R} + \lambda \sum_{\mathbf{h}} K_{\mathbf{h}} \operatorname{Im} \left\{ F_{\mathbf{h}}^{calc} \right\} \hat{\rho}_j^\dagger \hat{I}_{\mathbf{h},C} \right\} | \tilde{\varphi}_{j\beta} \rangle \quad (33)$$

to both sides of equation (31) and we obtain

$$\hat{F}^{j,exp} | \varphi_{j\beta} \rangle = \sum_{\gamma=1}^{n_j} \langle \varphi_{j\gamma} | \hat{F}^{j,exp} | \varphi_{j\beta} \rangle | \varphi_{j\gamma} \rangle \quad (34)$$

where $\hat{F}^{j,exp}$ is the modified "experimental" Fock operator for the fragment j :

$$\hat{F}^{j,exp} = \hat{F}^j + \lambda \sum_{\mathbf{h}} \hat{I}_{\mathbf{h},R}^j + \hat{I}_{\mathbf{h},C}^j \quad (35)$$

with

$$\hat{F}^j = (1 - \hat{\rho} + \hat{\rho}_j^\dagger) \hat{F} (1 - \hat{\rho} + \hat{\rho}_j) \quad (36)$$

$$\hat{I}_{\mathbf{h},R}^j = K_{\mathbf{h}} \operatorname{Re} \left\{ F_{\mathbf{h}}^{calc} \right\} (1 - \hat{\rho} + \hat{\rho}_j^\dagger) \hat{I}_{\mathbf{h},R} (1 - \hat{\rho} + \hat{\rho}_j) \quad (37)$$

$$\hat{I}_{\mathbf{h},C}^j = K_{\mathbf{h}} \operatorname{Im} \left\{ F_{\mathbf{h}}^{calc} \right\} (1 - \hat{\rho} + \hat{\rho}_j^\dagger) \hat{I}_{\mathbf{h},C} (1 - \hat{\rho} + \hat{\rho}_j) \quad (38)$$

Finally, given the invariance of the $\hat{F}^{j,exp}$ operator to a transformation that mixes only the

occupied ELMOs of each fragment among themselves, equations (34) can be rewritten in the following canonical form:

$$\hat{F}^{j,\exp} |\varphi'_{j\beta}\rangle = \epsilon_{j\beta} |\varphi'_{j\beta}\rangle \quad (39)$$

The XC-ELMO equations (39) are solved self-consistently for all the fragments. However, although solved separately, these equations are coupled due to the presence of the global density operator $\hat{\rho}$ in the definition of $\hat{F}^{j,\exp}$. Finally, it is worth noting that, in case of convergence problems associated with the intrinsic non-orthogonality of the ELMOs^{60,70,71}, we have also devised an alternative strategy for the direct minimisation of the functional J . This strategy relies on a quasi-Newton procedure that directly exploits first and second order derivatives of J with respect to the XC-ELMO coefficients^{57,58,71}.

Details About the X-Ray Constrained Calculations. We point out that the set of theoretical structure factor amplitudes $\left\{ |F_h^{calc}| \right\}$ is obtained taking into account the effects of the nuclear thermal motion. In particular, as already observed in Jayatilaka's and our previous works^{43,44,57,58}, since the structure factors are Fourier transforms of the unit-cell electron distribution, we can write

$$F_h^{calc} = \text{Tr} [\rho_0 \mathbf{I}_h] \quad (40)$$

with ρ_0 as the one-particle LCAO density matrix corresponding to the wave function of the reference crystal-unit and with \mathbf{I}_h as a matrix whose elements, in the atomic orbital basis, are given by this expression:

$$\left[\mathbf{I}_h \right]_{\mu\nu} = \sum_{k=1}^{N_m} e^{i2\pi \mathbf{r}_k \cdot (\mathbf{B}h)} T_{\mu\nu} \left[\mathbf{B}^{-1} \mathbf{R}_k^T \mathbf{B}h \right] \int d\mathbf{r} \chi_\mu(\mathbf{r}) \chi_\nu(\mathbf{r}) e^{i2\pi (\mathbf{R}_k \mathbf{r}) \cdot (\mathbf{B}h)} \quad (41)$$

where $T_{\mu\nu} \left[\mathbf{B}^{-1} \mathbf{R}_k^T \mathbf{B}h \right]$ is an empirical term that can have different functional forms^{21,72,73} and that depends on the thermal vibration parameters (namely, the Anisotropic Displace-

ment Parameters (or ADPs)) obtained experimentally for the atoms on which the basis functions $\chi_\mu(\mathbf{r})$ and $\chi_\nu(\mathbf{r})$ are centred.

Another important point is that, due to the experimental errors associated with the X-ray diffraction measurements, the χ^2 statistical agreement (see equation (4)) is not usually forced to zero, but the desired accuracy Δ (see equation (3)) is usually chosen equal to 1.0, so that the final computed structure factor amplitudes are on average within one standard deviation of the experimental data. Nevertheless, a common issue associated with the XC-calculations is that they do not always rapidly converge towards $\chi^2 = 1.0$. Different criteria have been proposed and adopted to halt the X-ray constrained procedure^{51,52,58}, but, unfortunately, this still remains an unsolved problem and an open field of research. In this paper we will use a strategy that we have introduced along with the XC-ELMO technique⁵⁸ and that consists in stopping the XC-calculations when one of the following three conditions are fulfilled:

$$\left\{ \begin{array}{l} \chi^2 < 1 \\ \frac{\chi_i^2 - \chi_{i-1}^2}{\lambda_i - \lambda_{i-1}} > -0.5 \\ \left| \frac{E_{\lambda_i}^{el} - E_{\lambda=0}^{el}}{E_{\lambda=0}^{el}} \right| > 5 \cdot 10^{-4} \end{array} \right. \quad (42)$$

While it is obvious that the first condition is the traditional one, the second and the third ones take into account the incremental ration of χ^2 with respect to the Lagrange multiplier λ and the percentage change of the electronic energy with respect to the unconstrained value, respectively. They have been proposed to prevent situations in which minimal improvements in the statistical agreement correspond to large values of the Lagrange multiplier and to large unphysical changes in the energy.

Computational Results

Preliminary Information. To show the performances of the techniques discussed in the previous section and to study the effects of the molecular orbitals localisation in the framework of the X-ray constrained wave function fitting, we have considered the crystallographic structure of the zwitterionic L-alanine determined by Destro *et al.* at 23 K⁷⁴. In particular, using the molecular geometry obtained from the diffraction experiment (see Figure 1), we have performed single point calculations at Restricted Hartree-Fock (RHF), ELMO, XC-RHF and XC-ELMO levels with six different basis-sets of increasing size and flexibility, namely the 3-21G, 6-31G(d), cc-pVDZ, 6-311G(d,p), aug-cc-pVDZ and 6-311++G(2d,2p) basis-sets. Furthermore, for all the ELMO and XC-ELMO computations we have adopted a localisation scheme almost corresponding to the Lewis structure of the system in exam. In fact, core and lone-pair electrons have been described considering atomic fragments, while almost all the bond electron-pairs have been treated resorting to bond subunits; the only exceptions are represented by the σ and π electrons of the carboxylic group for which the three-atom fragment C1-O5-O6 (see Figure 1) has been taken into account. For the "experimental" RHF and ELMO calculations we have also exploited the unit-cell parameters, the ADPs and the experimental structure factors amplitudes deposited by Destro and coworkers with their paper. Concerning the experimental diffraction data, which are not affected by serious secondary extinction effects and which had been previously corrected for scan-truncation losses, it is worth noting that only those characterised by $|F_{\mathbf{h}}^{\text{exp}}| > 3\sigma_{\mathbf{h}}$ have been selected for our computations, resulting into a set of 2435 structure factors amplitudes.

All the RHF and XC-RHF calculations have been performed using the TONTO package⁷⁵ developed by Jayatilka and coworkers, while each ELMO and XC-ELMO computation has been carried out exploiting the version 8 of the GAMESS-UK quantum chemistry suite of programs⁷⁶ that has been properly modified to implement both the original ELMO technique proposed by Stoll and the new X-ray constrained ELMO approach described in the previous section. Finally, the topological analyses of all the obtained electron distributions have been

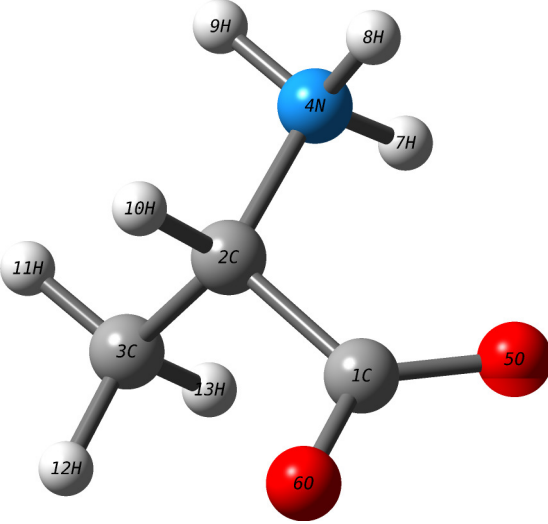


Figure 1: L-alanine molecular geometry obtained from the X-ray diffraction experiment.

performed by means of the version 13.11.04 of the AIMAll package⁷⁷.

Performance and Convergence of the Methods. In Table 1 we have reported the χ^2 and energy values obtained performing calculations on the L-alanine system. As expected, it is easy to observe that the X-ray constrained techniques always provide better statistical agreements with respect to the experimental data and that this agreement improves when larger and more flexible basis-sets are taken into account.

Nevertheless, despite the improved descriptions, even with the large 6-311++G(2d,2p) basis-set, we are not able to reach $\chi^2 = 1.0$. As already remarked in our previous papers^{58,59}, the difficulties in converging towards the desired agreement may be associated with errors in the collected experimental data. To better investigate this problem, we have analysed the normalised residuals $\left| \eta |F_{\mathbf{h}}^{calc}| - |F_{\mathbf{h}}^{exp}| \right| / \sigma_{\mathbf{h}}$ corresponding to all the experimentally constrained calculations. As we can observe in Figure 2, where we have reported the normalised residuals in function of the scattering resolution only for the 3-21G, 6-311G(d,p) and 6-311++G(2d,2p) basis-sets, a significant and systematic outlier occurs for all the XC-RHF and XC-ELMO computations at $\sin\theta/\lambda \approx 1.0 \text{ \AA}^{-1}$, being the normalised residual approximately equal to 10.8 in all the cases. Excluding the corresponding experimental value in

Table 1: χ^2 agreement statistics and energy values corresponding to all the unconstrained and constrained calculations performed on the L-alanine system. The λ_{max} value is shown for the constrained wave functions computations.

Method & Basis-Set	Unconstrained Calculations *		X-Ray Constrained Calculations		
	χ^2	Energy (a.u.)	λ_{max}	χ^2	Energy (a.u.)
<i>3-21G</i>					
RHF	4.43	-320.001	0.442	1.71	-319.841
ELMO	5.66	-319.850	0.580	2.29	-319.609
<i>6-31G(d)</i>					
RHF	2.53	-321.798	0.248	1.26	-321.747
ELMO	2.94	-321.696	0.320	1.30	-321.621
<i>cc-pVDZ</i>					
RHF	2.52	-321.831	0.240	1.23	-321.782
ELMO	3.02	-321.711	0.300	1.29	-321.640
<i>6-311G(d,p)</i>					
RHF	2.48	-321.891	0.230	1.21	-321.846
ELMO	2.94	-321.778	0.280	1.27	-321.712
<i>aug-cc-pVDZ</i>					
RHF	2.52	-321.863	0.230	1.20	-321.815
ELMO	2.74	-321.769	0.260	1.23	-321.712
<i>6-311++G(2d,2p)</i>					
RHF	2.47	-321.918	0.226	1.17	-321.873
ELMO	2.78	-321.830	0.280	1.19	-321.769

* The scale factors η have been optimised using the density matrices obtained from the unconstrained calculations.

the calculation of the statistical agreements for the basis-set 6-311++G(2d,2p), χ^2 further decreases to 1.12 and 1.14 for the XC-HF and XC-ELMO wave functions, respectively. This result further confirms that the impossibility of approaching the desired agreement is strictly related to the quality of the diffraction data used in the X-ray constrained calculations.

In Table 1 we can also note that all the RHF computations provide χ^2 values lower than those corresponding to the ELMO calculations. This is particularly evident in the unconstrained cases, whereas the discrepancy significantly reduces when X-ray constrained computations are performed. The observed trend can be ascribed to the effects of the experimental data that probably compensate for the quite strong approximation represented by the introduction of a pre-defined localisation scheme. Furthermore, we can easily see that the difference between the XC-RHF and XC-ELMO statistical agreements constantly decreases as more and more flexible basis-sets are used in the calculations, until a discrepancy of 0.02 is observed in the case of the 6-311++G(2d,2p) basis. This tendency can be also observed in Figure 3, where we have reported χ^2 trends corresponding to X-ray constrained RHF and X-ray constrained ELMO calculations carried out with three basis-sets of different size and quality: the quite small 3-21G basis-set (68 Atomic Orbitals (AOs) for the system in exam), the medium-size 6-311G(d,p) set of basis functions (156 AOs) and the large and flexible 6-311++G(2d,2p) basis (244 AOs). In fact, while in the 3-21G case the XC-RHF and XC-ELMO calculations converge to two different values (see Figure 3A), in the other two situations the XC-Hartree-Fock and XC-ELMO curves progressively approach the same limit (see Figure 3B and, especially, Figure 3C), which is not far from 1.0.

Further insights into the trends just discussed above can be obtained from a detailed analysis of the normalised residuals reported in Figure 2. Indeed, for the three basis sets taken into account, the number of outliers (i.e., normalised residuals greater than 3) is always lower for the XC-RHF wave functions: 65 against 116, 10 against 18 and 5 against 8 for the 3-21G, 6-311G(d,p) and 6-311++G(2d,2p) basis-sets, respectively. Moreover it is easy to observe that the discrepancy in the number of outliers between corresponding XC-RHF and

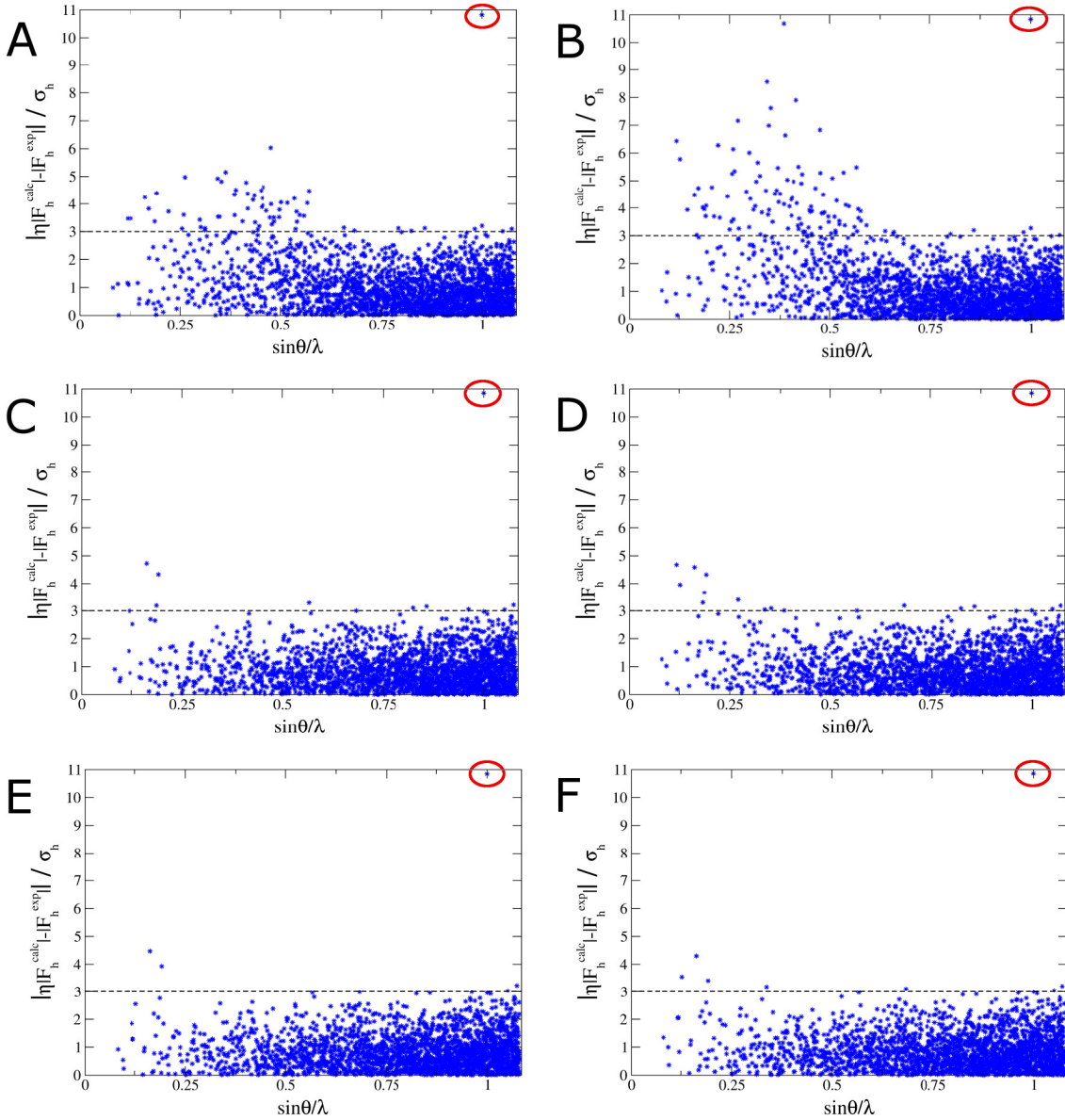


Figure 2: Normalised residuals of the structure factors amplitudes in function of the scattering resolution for the (A) XC-RHF/3-21G, (B) XC-ELMO/3-21G, (C) XC-RHF/6-311G(d,p), (D) XC-ELMO/6-311G(d,p), (E) XC-RHF/6-311++G(2d,2p) and (F) XC-ELMO/6-311++G(2d,2p) calculations. The horizontal dashed line represents the outliers-limit. The systematic outliers occurring at $\sin\theta/\lambda \approx 1.0 \text{ \AA}^{-1}$ are encircled.

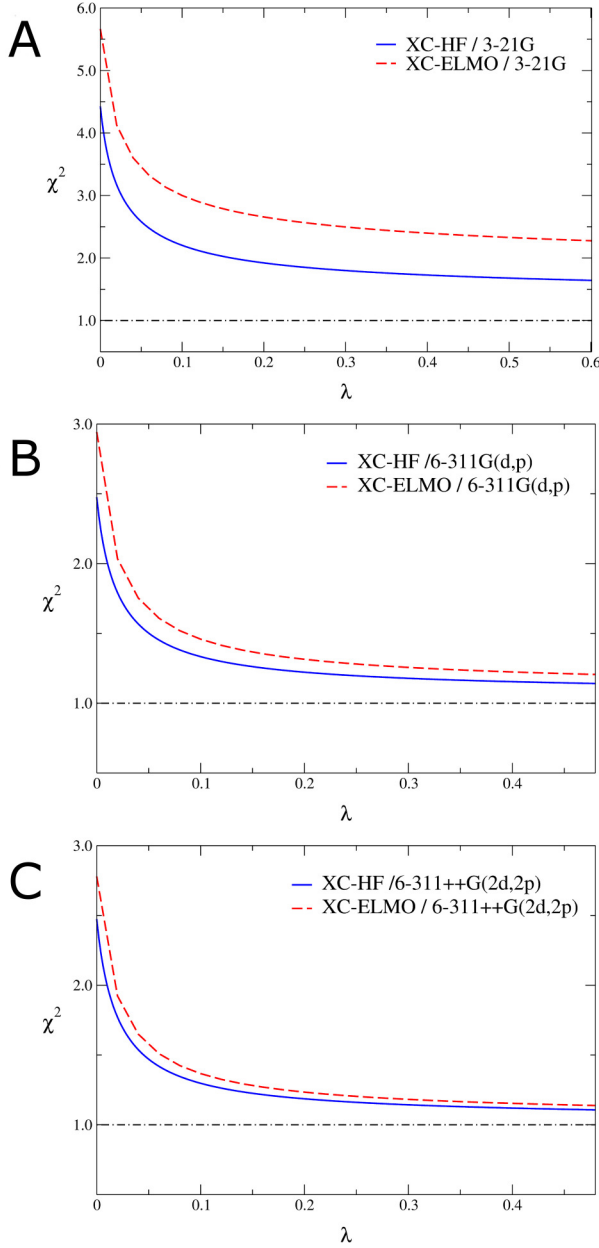


Figure 3: Variation of the χ^2 agreement statistics in function of the Lagrange multiplier λ for the XC-RHF and the XC-ELMO calculations when the (A) 3-21G, (B) 6-311G(d,p) and (C) 6-311++G(2d,2p) basis-sets are used. The solid (blue) and the dashed (red) lines represent the XC-RHF and XC-ELMO trends, respectively. The horizontal dash-and-dot line shows the desired statistical agreement.

XC-ELMO computations gradually reduces as the basis-set quality increases.

Therefore, all the results shown and discussed in this section seem to suggest that introducing a strict *a priori* localisation in experimentally constrained calculations can have a strong influence on the final results if small basis-sets are used. However, it also seems that, when higher quality basis-sets are considered, the bias coming from the pre-defined localisation becomes less important. In fact, in those cases, the more flexible basis-sets probably allow to capture most of the information coming from the experimental X-ray diffraction data, thus reducing the influence of the strict localisation constraints (namely, the localisation scheme) initially imposed on the electronic structure.

Before concluding this section, for the sake of completeness, we want to point out that all the energies associated with the X-ray constrained wave functions are higher than the energies obtained from the corresponding unconstrained computations. As already explained^{44,49,57}, this is the result of adding a constraint to the variational procedure without providing a new variational parameter.

Effects of the Localisation on the Charge Distributions. To further investigate the effects of introducing an *a priori* molecular orbitals localisation into the framework of the X-ray constrained wave function fitting, we have also analysed the electron densities obtained from the previously discussed calculations. To accomplish this task we have exploited the Quantum Theory of Atoms in Molecules (QTAIM)⁷⁸ and, for the sake of simplicity, we have considered only the charge distributions computed using the 3-21G, 6-311G(d,p) and 6-311++G(2d,2p) basis-sets. Furthermore, we have mainly focused on two of the main topological properties currently used in QTAIM charge density analyses: the electron density and its Laplacian at the bond critical points (BCPs). In particular, since our main goal was to study the influence of the imposed pre-localisation on the final electron distributions, we have determined the relative variations of the considered topological properties when the ELMO and XC-ELMO techniques have been used, considering the RHF and XC-RHF values

as references, respectively.

The relative variations of the electron density values at the bond critical points ($\rho(\mathbf{r}_b)$) are collected in Table 2. It is easy to observe that, both for unconstrained and X-ray constrained computations the use of Extremely Localised Molecular Orbitals does not entail significant changes, being the largest relative variation slightly larger than 4%. However, analysing the data obtained from the experimentally constrained calculations, it is worth noting that, in most of the cases, the relative variation reduces as the quality of the basis-set increases. Moreover, the lowest values are generally the ones corresponding to the flexible 6-311++G(2d,2p) basis. These remarks are even more interesting considering the fact that the same trends are no more observable when we examine the relative variations associated with the unconstrained computations. In fact, in those situations, the more flexible basis-sets 6-311G(d,p) and 6-311++G(2d,2p) are the ones for which we mainly observe the largest changes due to the introduction of the ELMOs.

Table 2: Unconstrained and X-ray constrained relative variations (U-RV and XC-RV, respectively) of the electron density values at the L-alanine bond critical points (BCPs).

BCPs	U-RV (%) *			XC-RV(%) *		
	3-21G	6-311G(d,p)	6-311++G(2d,2p)	3-21G	6-311G(d,p)	6-311++G(2d,2p)
N4-H7	-0.25	0.26	0.40	2.20	-1.55	-0.86
N4-H8	-0.19	0.16	0.33	-0.05	-0.30	-0.05
N4-H9	-0.65	0.29	0.29	3.82	1.99	0.69
N4-C2	0.48	-0.01	0.99	0.66	-0.19	0.23
C2-H10	0.36	1.85	1.50	-0.57	-0.08	-0.55
C2-C3	-0.96	1.56	1.33	-0.38	0.46	0.00
C3-H11	-0.16	0.26	0.39	-0.23	0.14	-0.11
C3-H12	-0.05	0.16	0.49	1.53	0.69	-0.03
C3-H13	0.04	0.23	0.41	1.15	-0.03	-0.36
C2-C1	-0.42	3.54	2.81	-0.56	1.33	0.82
C1-O5	1.95	2.02	1.84	4.22	2.38	2.04
C1-O6	1.73	1.97	1.93	2.74	2.05	1.89

* U-RV(%) = 100.0 (ELMO – RHF)/RHF; XC-RV(%) = 100.0 (XC-ELMO – XC-RHF)/XC-RHF

In Table 3 we have reported the relative variations of the Laplacian values at the bond critical points. Unlike the previous case, it is possible to note a larger variability that was actually expected due to the extreme sensitivity of the Laplacian to the position of the BCPs. Nevertheless, also for this topological property we observe the same trends of Table 2. In fact, considering the data corresponding to the X-ray constrained calculations, the lowest relative variations are mainly obtained when the 6-311++G(2d,2p) basis-set is taken into account while, focusing on the unconstrained computations, the more flexible basis-sets (i.e., 6-311G(d,p) and 6-311++G(2d,2p)) generally provide the largest relative changes.

Table 3: Unconstrained and X-ray constrained relative variations (U-RV and XC-RV, respectively) of the Laplacian values of the electron density at the L-alanine bond critical points (BCPs).

BCPs	U-RV (%) *			XC-RV(%) *		
	3-21G	6-311G(d,p)	6-311++G(2d,2p)	3-21G	6-311G(d,p)	6-311++G(2d,2p)
N4-H7	-0.38	0.54	0.50	2.14	0.56	0.97
N4-H8	0.03	0.37	0.38	-1.03	1.52	0.75
N4-H9	-0.94	1.56	0.74	-1.87	2.84	0.44
N4-C2	54.37	-2.26	31.29	9.28	0.21	3.49
C2-H10	0.81	3.88	2.82	0.66	2.00	0.30
C2-C3	0.03	7.88	6.66	0.13	5.50	3.62
C3-H11	-0.68	0.95	1.19	-0.18	1.31	1.04
C3-H12	-0.71	0.09	1.27	1.46	1.52	0.81
C3-H13	-0.45	0.60	1.21	1.62	0.60	-0.60
C2-C1	8.26	14.89	11.01	9.41	8.56	6.58
C1-O5	27.64	93.78	50.44	44.53	29.90	28.79
C1-O6	16.90	47.87	37.20	20.93	18.95	20.44

* U-RV(%) = 100.0 (ELMO – RHF)/RHF; XC-RV(%) = 100.0 (XC-ELMO – XC-RHF)/XC-RHF

The trends observed for the relative variations of the topological properties are in line with the results discussed in the previous section. In fact, from Tables 2 and 3 we can infer that the use of Extremely Localised Molecular Orbitals in X-ray constrained calculations determines larger changes in the electron density properties only when small basis-sets are used. On the contrary, when we employ larger and more flexible sets of basis functions, the

influence of the pre-defined localisation on the electron distribution becomes less significant.

Conclusions and Perspectives

Nowadays, the experimentally constrained wave function approaches represent an alternative to the very well known *ab initio* and DFT methods. Although several researchers have been working on this subject for almost five decades, the field is largely unexplored and new interesting developments are still possible. New advances in this area of research will be beneficial not only to the quantum chemistry community, but also to experimental researchers. In fact, if on the one hand new strategies could help to shed light on crucial theoretical problems (e.g., the Hohenberg & Kohn mapping between electron densities and wave functions), on the other hand new methods could also become valuable tools for the direct interpretation of experimental data.

In this paper we focused our attention on the X-ray constrained wave function fitting proposed by Jayatilaka. This technique is probably the most promising among all the "experimental" wave function strategies and it is currently considered as a quantum mechanically rigorous method to reconstruct charge distributions in crystals from experimental diffraction data. Nevertheless, due to the complete delocalisation of the obtained Molecular Orbitals, this method is not characterised by an immediate chemical interpretability in terms of the traditional Lewis molecular picture. To recover it, the strategy has been recently extended in order to obtain molecular orbitals strictly localised on small molecular fragments (e.g., atoms, bonds or functional groups) from experimental X-ray diffraction data by defining *a priori* localisation schemes that, however, represent strong initial assumptions about the electronic structure of the systems in exam.

In order to evaluate to what extent these assumptions impact on the obtained electron densities, here we have compared results obtained through "traditional" X-ray constrained Hartree-Fock calculations to results of X-ray constrained ELMO computations. Analysing

statistical agreements with the experimental data, convergence trends and also topological properties of charge distributions, we have observed that, if small basis-sets are used in the calculations, the *a priori* localisation of the molecular orbitals has indeed a strong influence on the final electron densities. Nevertheless, employing larger sets of basis functions, the XC-HF and XC-ELMO calculations tend to more similar results. This can be explained considering that the flexibility of larger and larger basis-sets allows to increasingly exploit the information provided by the experimental data and, consequently, to gradually mitigate the initial bias represented by the pre-defined localisation. **Therefore, when adequate basis-sets are used, the introduction of a localisation scheme represents a less severe approximation and it allows to directly include traditional chemical concepts in the X-ray constrained wave function fitting.**

However, in order to further improve the X-ray constrained wave function approaches, some open questions must be still addressed. For instance, as already mentioned in the Theory section, a definitive and sound criterion to halt the X-ray constrained procedure should be defined. Furthermore, it will be crucial to perform detailed studies to understand if the X-ray constrained wave functions are really able to capture both the electron correlation and the crystal field effects, which are intrinsically included in the experimental diffraction data. Besides these important problems, in our research group we are also considering the possibility of extending Jayatilaka's approach to a multi-determinant wave function ansatz since, until now, only single Slater determinants have been considered.

Finally, concerning the more recent XC-ELMO technique, we are currently exploiting the reliable transferability of the Extremely Localised Molecular Orbitals^{79–81} to construct original libraries of XC-ELMOs. They could become an alternative to the existing pseudoatoms databases^{82–87} that have been already successfully used in the framework of the multipole model techniques to refine crystallographic structures and to determine electrostatic properties of macromolecular systems.

Acknowledgement

The CNRS and the University of Lorraine (PEPS Mirabelle project "KiteComb") and the Institute Jean Barriol of the University of Lorraine (Axe-R12 project) are gratefully acknowledged for financial support.

References

- (1) Hohenberg, P.; Kohn, W. Inhomogeneous Electron Gas. *Phys. Rev. B* **1964**, *36*, 864–871.
- (2) Hirshfeld, F. L. Difference Densities by Least-Squares Refinement: Fumaramic Acid. *Acta Cryst. B* **1971**, *27*, 769–781.
- (3) Stewart, R. F. Electron Population Analysis with Rigid Pseudoatoms. *Acta Cryst. A* **1976**, *32*, 565–574.
- (4) Hansen, N. K.; Coppens, P. Testing Aspherical Atom Refinements on Small-Molecule Data Sets. *Acta Cryst. A* **1978**, *34*, 909–921.
- (5) Mukherji, A.; Karplus, M. Constrained molecular wavefunctions: HF molecule. *J. Chem. Phys.* **1963**, *38*, 44–48.
- (6) Rasiel, Y.; Whitman, D. R. Constrained-variation method in molecular quantum mechanics. *J. Chem. Phys.* **1965**, *42*, 2124–2131.
- (7) Chong, D. P.; Byers-Brown, W. Perturbation theory of constraints: application to a lithium hydride calculation. *J. Chem. Phys.* **1966**, *45*, 392–395.
- (8) Chong, D. P.; Rasiel, Y. Constrained-variation method in molecular quantum mechanics. Comparison of different approaches. *J. Chem. Phys.* **1966**, *44*, 1819–1823.
- (9) Clinton, W. L.; Nakhleh, J.; Wunderlich, F. Direct Determination of Pure-State Density Matrices. I. Some Simple Introductory Calculations. *Phys. Rev.* **1969**, *177*, 1–6.
- (10) Clinton, W. L.; Galli, A. J.; Massa, L. J. Direct Determination of Pure-State Density Matrices. II. Construction of Constrained Idempotent One-Body Densities. *Phys. Rev.* **1969**, *177*, 7–13.

- (11) Clinton, W. L.; Henderson, G. A.; Prestia, J. V. Direct Determination of Pure-State Density Matrices. III. Purely Theoretical Densities Via an Electrostatic-Virial Theorem. *Phys. Rev.* **1969**, *177*, 13–18.
- (12) Clinton, W. L.; Lamers, G. B. Direct Determination of Pure-State Density Matrices. IV. Investigation of Another Constraint and Another Application of the P Equations. *Phys. Rev.* **1969**, *177*, 19–27.
- (13) Clinton, W. L.; Galli, A. J.; Henderson, G. A.; Lamers, G. B.; Massa, L. J.; Zarur, J. Direct Determination of Pure-State Density Matrices. V. Constrained Eigenvalue Problems. *Phys. Rev.* **1969**, *177*, 27–33.
- (14) Clinton, W. L.; Massa, L. J. Determination of the Electron Density Matrix from X-Ray Diffraction Data. *Phys. Rev. Lett.* **1972**, *29*, 1363–1366.
- (15) Clinton, W. L.; Frishberg, C. A.; Massa, L. J.; Oldfield, P. A. Methods for Obtaining an Electron-Density Matrix from X-Ray Diffraction Data. *Int. J. Quantum Chem. Symp.* **1973**, *7*, 505–514.
- (16) Frishberg, C.; Massa, L. J. Idempotent Density Matrices for Correlated Systems from X-Ray Diffraction Structure Factors. *Phys. Rev. B* **1981**, *24*, 7018–7024.
- (17) Pecora, L. M. Determination of the quantum density matrix from experiment: An application to positron annihilation. *Phys. Rev. B* **1986**, *33*, 5987–5993.
- (18) Massa, L.; Goldberg, M.; Frishberg, C.; Boehme, R. F.; Placa, S. J. L. Wave Functions Derived by Quantum Modeling of the Electron Density from Coherent X-Ray Diffraction: Beryllium Metal. *Phys. Rev. Lett.* **1985**, *55*, 622–625.
- (19) Howard, S. T.; Huke, J. P.; Mallinson, P. R.; Frampton, C. S. Density Matrix Refinement for Molecular Crystals. *Phys. Rev. B* **1994**, *49*, 7124–7136.

- (20) Snyder, J. A.; Stevens, E. D. A Wavefunction and Energy of the Azide Ion in Potassium Azide Obtained by a Quantum-Mechanically Constrained Fit to X-Ray Diffraction Data. *Chem. Phys. Lett.* **1999**, *313*, 293–298.
- (21) Tanaka, K. X-ray analysis of wavefunctions by the least-squares method incorporating orthonormality. I. General formalism. *Acta Cryst. A* **1988**, *44*, 1002–1008.
- (22) Tanaka, K.; Makita, R.; Funahashi, S.; Komori, T.; Win, Z. X-ray atomic orbital analysis. I. Quantum-mechanical and crystallographic framework of the method. *Acta Cryst. A* **2008**, *64*, 437–449.
- (23) Hibbs, D. E.; Howard, S. T.; Huke, J. P.; Waller, M. P. A New Orbital-Based Model for the Analysis of Experimental Molecular Charge Densities: an Application to (Z)-N-Methyl-C-Phenylnitrone. *Phys. Chem. Chem. Phys.* **2005**, *7*, 1772–1778.
- (24) Waller, M. P.; Howard, S. T.; Platts, J. A.; Piltz, R. O.; Willock, D. J.; Hibbs, D. E. Novel Properties from Experimental Charge Densities: an Application to the Zwitterionic Neurotransmitter Taurine. *Chem. Eur. J.* **2006**, *12*, 7603–7614.
- (25) Schmider, H.; Smith, V. H.; Weyrich, W. Determination of electron densities and one-matrices from experimental information. *Trans. Am. Crystal. Assoc.* **1990**, *26*, 125–140.
- (26) Schmider, H.; Smith, V. H.; Weyrich, W. Reconstruction of the one-particle density matrix from expectation values in position and momentum space. *J. Chem. Phys.* **1992**, *96*, 8986–8994.
- (27) Weyrich, W. An electronic position and momentum density study of chemical bonding in TiO₂ (Rutile). *Lect. Ser. Comput. Comput. Sci.* **2006**, *5*, 1–3.
- (28) Gillet, J.-M.; Becker, P. J. Position and momentum densities. Complementarity at work: refining a quantum model from different data sets. *J. Phys. Chem. Sol.* **2004**, *65*, 2017–2023.

- (29) Gillet, J.-M. Determination of a one-electron reduced density matrix using a coupled pseudo-atom model and a set of complementary scattering data. *Acta Cryst. A* **2007**, *63*, 234–238.
- (30) Gillet, J.-M.; Becker, P. J.; Cortona, P. Joint refinement of a local wave-function model from Compton and Bragg scattering data. *Phys. Rev. B* **2001**, *63*, 235115.
- (31) Cooper, M. Compton scattering and electron momentum determination. *Rep. Prog. Phys.* **1985**, *48*, 415–481.
- (32) Loupias, G.; Chomilier, J. Electron momentum density and Compton profiles: an accurate check of overlap models. *Z. Phys. D: Atoms Mol. Clust.* **1986**, *2*, 297–308.
- (33) Cassam-Chenaï, P. Ensemble Representable Densities for Atoms and Molecules. I. General Theory. *Int. J. Quantum Chem.* **1995**, *54*, 201–210.
- (34) Cassam-Chenaï, P.; Wolff, S.; Chandler, G.; Figgis, B. Ensemble-representable densities for atoms and molecules. II. Application to CoCl_4^{2-} . *Int. J. Quantum Chem.* **1996**, *60*, 667–680.
- (35) Gilbert, T. L. Hohenberg-Kohn theorem for nonlocal external potentials. *Phys. Rev. B* **1975**, *12*, 2111–2120.
- (36) Henderson, G. A.; Zimmerman, R. K. One-electron properties as variational parameters. *J. Chem. Phys.* **1976**, *65*, 619–622.
- (37) Levy, M.; Goldstein, J. A. Electron density-functional theory and x-ray structure factors. *Phys. Rev. B* **1987**, *35*, 7887–7890.
- (38) Gritsenko, O. V.; Zhidomirov, G. M. On the determination of the 1st-order density-matrix from the diffraction experiment data. *Dokl. Akad. Nauk. SSSR* **1987**, *293*, 1162–1166.

- (39) Zhao, Q.; Parr, R. G. Quantities $T_s[n]$ and $T_c[n]$ in density functional theory. *Phys. Rev. A* **1992**, *46*, 2337–2343.
- (40) Zhao, Q.; Parr, R. G. Constrained-search method to determine electronic wave functions from electronic densities. *J. Chem. Phys.* **1993**, *98*, 543–548.
- (41) Zhao, Q.; Morrison, R. C.; Parr, R. G. From electron densities to Kohn-Sham kinetic energies, orbital energies, exchange-correlation potentials, and exchange correlation energies. *Phys. Rev. A* **1994**, *50*, 2138–2142.
- (42) Levy, M. Universal variational functionals of electron densities, first-order density matrices, and natural spin-orbitals and solution of the v-representability problem. *Proc. Natl Acad. Sci. USA* **1979**, *76*, 6062–6065.
- (43) Jayatilaka, D. Wave Function for Beryllium from X-Ray Diffraction Data. *Phys. Rev. Lett.* **1998**, *80*, 798–801.
- (44) Jayatilaka, D.; Grimwood, D. J. Wavefunctions Derived from Experiment. I. Motivation and Theory. *Acta Cryst. A* **2001**, *57*, 76–86.
- (45) Grimwood, D. J.; Jayatilaka, D. Wavefunctions Derived from Experiment. II. A Wavefunction for Oxalic Acid Dihydrate. *Acta Cryst. A* **2001**, *57*, 87–100.
- (46) Bytheway, I.; Grimwood, D.; Jayatilaka, D. Wavefunctions Derived from Experiment. III. Topological Analysis of Crystal Fragments. *Acta Cryst. A* **2002**, *58*, 232–243.
- (47) Bytheway, I.; Grimwood, D. J.; Figgis, B. N.; Chandler, G. S.; Jayatiaka, D. Wavefunctions Derived from Experiment. IV. Investigation of the Crystal Environment of Ammonia. *Acta Cryst. A* **2002**, *58*, 244–251.
- (48) Grimwood, D. J.; Bytheway, I.; Jayatilaka, D. Wavefunctions Derived from Experiment. V. Investigation of Electron Densities, Electrostatic Potentials, and Electron

Localization Functions for Noncentrosymmetric Crystals. *J. Comput. Chem.* **2003**, *24*, 470–483.

- (49) Hudák, M.; Jayatilaka, D.; Peraínova, L.; Biskupic, S.; Kozísek, J.; Bucinský, L. X-Ray Constrained Unrestricted Hartree-Fock and Douglas-Kroll-Hess Wavefunctions. *Acta Cryst. A* **2010**, *66*, 78–92.
- (50) Jayatilaka, D. *Using Wavefunctions to Get More Information Out of Diffraction Experiments* in: *Modern Charge-Density Analysis* (Editors: C. Gatti and P. Macchi); Springer: Berlin, 2012; pp 213–257.
- (51) Whitten, A. E.; Jayatilaka, D.; Spackman, M. Effective molecular polarizabilities and crystal refractive indices estimated from x-ray diffraction data. *J. Chem. Phys.* **2006**, *125*, 174505.
- (52) Hickstein, D. D.; Cole, J. M.; Turner, M. J.; Jayatilaka, D. Modeling electron density distributions from X-ray diffraction to derive optical properties: Constrained wavefunction versus multipole refinement. *J. Chem. Phys.* **2013**, *139*, 064108.
- (53) Jayatilaka, D.; Grimwood, D. Electron Localization Functions Obtained from X-Ray Constrained Hartree-Fock Wavefunctions for Molecular Crystals of Ammonia, Urea and Alloxan. *Acta Cryst. A* **2004**, *60*, 111–119.
- (54) Grabowsky, S.; Jayatilaka, D.; Mebs, S.; Luger, P. The Electron Localizability Indicator from X-Ray Diffraction Data - A First Application to a Series of Epoxide Derivatives. *Chem. Eur. J.* **2010**, *16*, 12818–12821.
- (55) Grabowsky, S.; Weber, M.; Jayatilaka, D.; Chen, Y.-S.; Grabowski, M. T.; Brehme, R.; Hesse, M.; Schirmeister, T.; Luger, P. Reactivity Differences between α,β -Unsaturated Carbonyls and Hydrazones Investigated by Experimental and Theoretical Electron Density and Electron Localizability Analyses. *J. Phys. Chem. A* **2011**, *115*, 12715–12732.

- (56) Grabowsky, S.; Luger, P.; Buschmann, J.; Schneider, T.; Schirmeister, T.; Sobolev, A. N.; Jayatilaka, D. The Significance of Ionic Bonding in Sulfur Dioxide: Bond Orders from X-ray Diffraction Data. *Angew. Chem. Int. Ed.* **2012**, *51*, 6776–6779.
- (57) Genoni, A. Molecular Orbitals Strictly Localized on Small Molecular Fragments from X-Ray Diffraction Data. *J. Phys. Chem. Lett.* **2013**, *4*, 1093–1099.
- (58) Genoni, A. X-ray Constrained Extremely Localized Molecular Orbitals: Theory and Critical Assessment of the New Technique. *J. Chem. Theory Comput.* **2013**, *9*, 3004–3019.
- (59) dos Santos, L. H. R.; Genoni, A.; Macchi, P. Unconstrained and X-ray constrained extremely localized molecular orbitals: analysis of the reconstructed electron density. *Acta Cryst. A* **2014**, *70*, 532–551.
- (60) Stoll, H.; Wagenblast, G.; Preuss, H. On the Use of Local Basis Sets for Localized Molecular Orbitals. *Theoret. Chim. Acta* **1980**, *57*, 169–178.
- (61) Pipek, J.; Mezey, P. G. A fast intrinsic localization procedure applicable for ab initio and semiempirical linear combination of atomic orbital wave functions. *J. Chem. Phys.* **1989**, *90*, 4916–4926.
- (62) Boys, S. F. Construction of Some Molecular Orbitals to Be Approximately Invariant for Changes from One Molecule to Another. *Rev. Mod. Phys.* **1960**, *32*, 296–299.
- (63) Foster, J. M.; Boys, S. F. Canonical Configurational Interaction Procedure. *Rev. Mod. Phys.* **1960**, *32*, 300–302.
- (64) Edmiston, C.; Ruedenberg, K. Localized Atomic and Molecular Orbitals. *Rev. Mod. Phys.* **1963**, *35*, 457–465.

- (65) Edmiston, C.; Ruedenberg, K. Localized Atomic and Molecular Orbitals. II. *J. Chem. Phys.* **1965**, *43*, s97–S116.
- (66) Becke, A. D.; Edgecombe, K. E. A simple measure of electron localization in atomic and molecular systems. *J. Chem. Phys.* **1990**, *92*, 5397–5403.
- (67) Kohout, M. A Measure of Electron Localizability. *Int. J. Quantum Chem.* **2004**, *97*, 651–658.
- (68) Genoni, A.; Sironi, M. A novel approach to relax extremely localized molecular orbitals: the extremely localized molecular orbital?valence bond method. *Theor. Chem. Acc.* **2004**, *112*, 254–262.
- (69) Genoni, A.; Fornili, A.; Sironi, M. Optimal Virtual Orbitals to Relax Wave Functions Built Up with Transferred Extremely Localized Molecular Orbitals. *J. Comput. Chem.* **2005**, *26*, 827–835.
- (70) Smits, G. F.; Altona, C. Calculation and Properties of Non-Orthogonal, Strictly Local Molecular Orbitals. *Theoret. Chim. Acta* **1985**, *67*, 461–475.
- (71) Fornili, A.; Sironi, M.; Raimondi, M. Determination of Extremely Localized Molecular Orbitals and Their Application to Quantum Mechanics/Molecular Mechanics Methods and to the Study of Intramolecular Hydrogen Bonding. *J. Mol. Struct. (Theochem)* **2003**, *632*, 157–172.
- (72) Stewart, R. F. Generalized X-Ray Scattering Factors. *J. Chem. Phys.* **1969**, *51*, 4569–4577.
- (73) Coppens, P.; Willoughby, T. V.; Csonka, L. N. Electron population analysis of accurate diffraction data. I. Formalisms and restrictions. *Acta Cryst. A* **1971**, *27*, 248–256.
- (74) Destro, R.; Marsh, R. E.; Bianchi, R. A low-temperature (23-K) study of L-alanine. *J. Phys. Chem.* **1988**, *92*, 966–973.

- (75) Jayatilaka, D.; Grimwood, D. J. Tonto: A Fortran Based Object-Oriented System for Quantum Chemistry and Crystallography. *Computational Science - ICCS 2003. Lecture Notes in Computer Science* **2003**, *2660*, 142–151.
- (76) Guest, M. F.; Bush, I. J.; van Dam, H. J. J.; Sherwood, P.; Thomas, J. M. H.; van Lenthe, J. H.; Havenith, R. W. A.; Kendrick, J. The GAMESS-UK Electronic Structure Package: Algorithms, Developments and Applications. *Mol. Phys.* **2005**, *103*, 719–747.
- (77) Keith, T. A. *AIMAll (Version 13.11.04)*; TK Gristmill Software: Overland Park, KS, U.S.A. (aim.tkgristmill.com), 2012.
- (78) Bader, R. F. W. *Atoms in Molecules: a Quantum Theory*; Oxford University Press, 1990.
- (79) Genoni, A.; Ghitti, M.; Pieraccini, S.; Sironi, M. A Novel Extremely Localized Molecular Orbitals Based Technique for the One-Electron Density Matrix Computation. *Chem. Phys. Lett.* **2005**, *415*, 256–260.
- (80) Sironi, M.; Genoni, A.; Civera, M.; Pieraccini, S.; Ghitti, M. Extremely Localized Molecular Orbitals: Theory and Applications. *Theor. Chem. Acc.* **2007**, *117*, 685–698.
- (81) Sironi, M.; Ghitti, M.; Genoni, A.; Saladino, G.; Pieraccini, S. DENPOL: a New Program to Determine Electron Densities of Polypeptides Using Extremely Localized Molecular Orbitals. *J. Mol. Struct. (Theochem)* **2009**, *898*, 8–16.
- (82) Pichon-Pesme, V.; Lecomte, C.; Lachekar, H. On Building a Data Bank of Transferable Experimental Electron Density Parameters: Application to Polypeptides. *J. Phys. Chem* **1995**, *99*, 6242–6250.
- (83) Zarychta, B.; Pichon-Pesme, V.; Guillot, B.; Lecomte, C.; Jelsch, C. On the Application of an Experimental Multipolar Pseudo-Atom Library for Accurate Refinement of Small-Molecule and Protein Crystal Structures. *Acta Cryst. A* **2007**, *63*, 108–125.

- (84) Koritsanszky, T.; Volkov, A.; Coppens, P. Aspherical-Atom Scattering Factors from Molecular Wave Functions. 1. Transferability and Conformation Dependence of Atomic Electron Densities of Peptides within the Multipole Formalism. *Acta Cryst A* **2002**, *58*, 464–472.
- (85) Volkov, A.; Li, X.; Koritsanszky, T.; Coppens, P. Ab Initio Quality Electrostatic Atomic and Molecular Properties Including Intermolecular Energies from a Transferable Theoretical Pseudoatom Databank. *J. Phys. Chem. A* **2004**, *108*, 4283–4300.
- (86) Dittrich, B.; Koritsanszky, T.; Luger, P. A Simple Approach to Nonspherical Electron Densities by Using Invarioms. *Angew. Chem. Int. Ed.* **2004**, *43*, 2718–2721.
- (87) Dittrich, B.; Hübschle, C. B.; Luger, P.; Spackman, M. A. Introduction and Validation of an Invariom Database for Amino-Acid, Peptide and Protein Molecules. *Acta Cryst. D* **2006**, *62*, 1325–1335.